PETROLOGY =

Late Cretaceous Rapakivi Granites and Associating Rocks in the Evolution of the Okhotsk-Chukotka Active Margin

A. E. Vernikovskaya^{a,b,c}, Corresponding member of the RAS V. Yu. Fridovsky^c, N. Yu. Matushkin^{a,b,*}, Ya. A. Tarasov^c, E. A. Bogdanov^{a,b}, N. V. Rodionov^d, and P. I. Kadilnikov^{a,b†}

^aNovosibirsk State University, Novosibirsk, 630090 Russia
^bTrofimuk Institute of Petroleum Geology and Geophysics Novosibirsk, 630090 Russia
^cDiamond and Precious Metal Geology Institute, Yakutsk, 677000 Russia
^dAll-Russian Geological Research Institute of A.P. Karpinsky, St. Petersburg, 199106 Russia
*e-mail: matushkinny@ipgg.sbras.ru
Received May 23, 2025; revised June 16, 2025; accepted June 23, 2025

Abstract—We report new data on the mineralogy, petrography, geochemistry, U—Th—Pb geochronology, and Sm—Nd and Rb—Sr isotopy of granitoids and associating rocks of the Sup, Duzunya and Batyrchan plutons, including rocks with rapakivi texture, which we combine into the new Severookhotsk complex. These rocks were formed in the Cenomanian—Coniacian ages 94–88 Ma (U—Pb SHRIMP-II data) in the back-arc of the West Okhotsk flank zone of the Okhotsk-Chukotka volcanoplutonic belt. Sm—Nd and Rb—Sr isotopic data confirm the presence of both an enriched mantle and a continental crust component in the composition of the magmatic source of the rapakivi granites. We show that the Severookhotsk complex magmatism and the Sn-polymetallic and Au—Bi mineralization of the Allakh-Yun tectonic zone have the same origin.

Keywords: granite, monzonite, rapakivi, geochemistry, U—Th—Pb geochronology, southeastern margin of Northern Asia, Verkhoyansk-Chukotka folded area, Okhotsk-Chukotka volcanoplutonic belt, active continental margin, Late Cretaceous

DOI: 10.1134/S1028334X25608004

INTRODUCTION

The Mesozoic interval of the development of the southeastern margin of North Asia (Verkhoyansk-Chukotka folded area) was marked by several stages of an evolving subduction zone due to the closing of the Mongol-Okhotsk, Paleopacific, and Pacific oceans [1-3]. During the late Permian—Early Cretaceous interval, the Uda-Murgal convergent boundary was developing, as an active continental margin in its southwestern part [2, 4, 5]. During the Aptian age, rapakivi granites and associating mafic dikes with U-Pb ages ~120 Ma formed in the back-arc and localized-in the Allakh-Yun tectonic zone of the South Verkhoyansk sector of the Verkhoyansk fold-andthrust belt (VFTB) [6, 7]. This magmatic activity marked the beginning of the transformation of the convergent boundaries in the evolution of southeastern margin of Northern Asia and, like other rapakivibearing subduction formations (e.g., [8]), are evidence of slab failure. During the Albian-Campanian stage the Okhotsk-Chukotka active margin formed along the entire southwestern boundary of the Verkhovansk-Chukotka folded area. The age of the Okhotsk-Chu-

Here we present results of new integrated mineralogical, petrographic, geochronological (U-Pb, SHRIMP-II), isotope (Sm-Nd, Rb-Sr), and geochemical (ICP-MS) investigations directed at studying the age, origin and geodynamic formation conditions of acid and intermediate rocks including rapakivi granites of the Sup, Duzunya, and Batyrchan plutons that are located in the back-arc of the West Okhotsk flank sector of the OCVB. These plutons intruded ter-

kotka volcanoplutonic belt (OCVB) magmatism is in the range 109–76 Ma based on U–Pb and ⁴⁰Ar/³⁹Ar geochronological data and biostratigraphy (reviewed in [9, 10]). These data show the decreasing age of magmatism in the axial zone (volcanic arc) of the OCVB from the southwest to the northeast-from 109-94 Ma in the West Okhotsk flank sector to 99-80 Ma in the Okhotsk and Central Chukotka sectors to 91-76 Ma in the East Chukotka flank sector. Of special interest is the study of the connection between the origins of this magmatism and the coeval mineralization of the largest deposits that reflect overlapping tectonothermal events in the Cenomanian age (100–94 Ma, ⁴⁰Ar/³⁹Ar method). These include the Sn-polymetallic Kuta (100 Ma) and Au-Bi Kurum (95 Ma) deposits located in the Allakh-Yun tectonic zone [11, 12].

[†] Deceased.

35 Page 2 of 9 VERNIKOVSKAYA et al.

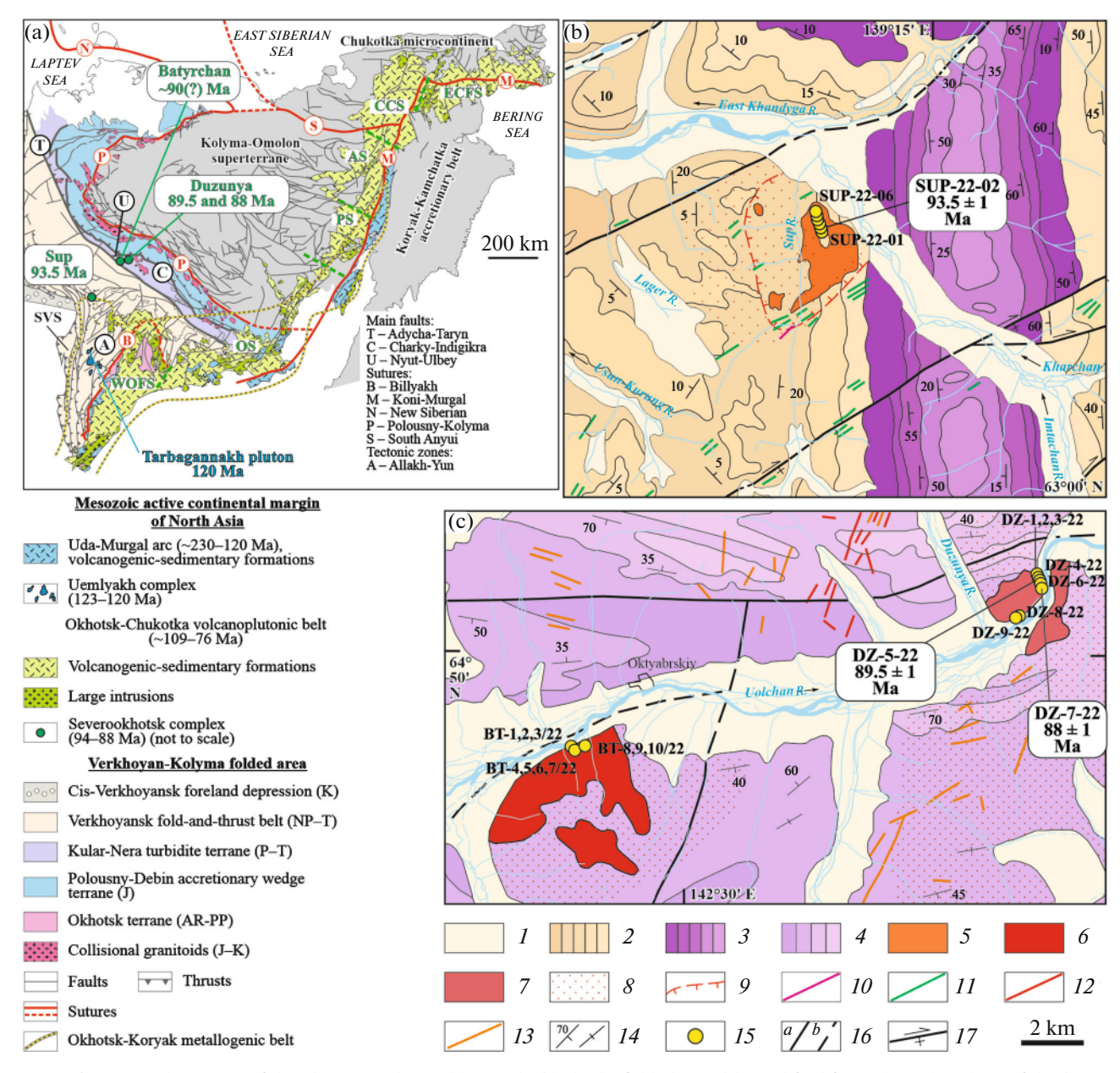


Fig. 1. Regional position of the plutons in the Verkhoyansk-Chukotka folded area (a) modified from [8] and geology of the Sup (b) and Batyrchan and Duzunya plutons (c) simplified from materials of state geological mapping at scale 1: 200000 [13, 14]. I, alluvium, glacial, and glaciofluvial deposits (Q); 2, siltstone, sandstone, conglomerate, basaltic and acidic tuff (P_2); 3, sandstone, siltstone, mudstone, gritstone, conglomerate (T_{1-2}); 4, siltstone, sandstone, lenses of slump breccia (T_3); 5-7, plutons of the Severookhotsk complex (94–88 Ma): 5, Sup, monzodiorite, quartz monzonite, granodiorite; 6, Batyrchan, low-alkaline granite, granite, subalkaline granite; 7, Duzunya, granodiorite, granite, low-alkaline granite, leucocratic granite, subalkaline granite, including rapakivi varieties; 8, contact hornfels and hornfelsed rock; 9, boundaries of the cordierite contact metamorphism zone; 10-13, dikes: 10, monzodiorite (K_1); 11, dolerite, diorite, monzonite and lamprophyre (K_{1-2}); 12, granite porphyry (K_1); 13, diorite-porphyry, andesibasalt, andesite, and rhyolite (13); 14, inclined and vertical bedding attitude; 15, sampling sites; 16, identified (a) and inferred (b) faults; 17, reverse faults with dextral strike-slip. Sectors of the OCVB from [10] (green dashed lines are their boundaries): WOFS—West Okhotsk flank sector; OS—Okhotsk sector; PS—Penzhina sector; AS—Anadyr sector; CCS—Central Chukotka sector; ECFS—East Chukotka flank sector. SVS—South Verkhoyansk sector of the VFTB.

rigenous deposits of different blocks of the southeastern passive continental margin of the Siberian craton, namely the South Verkhoyansk sector (SVS) and the Kular-Nera terrane and associate with the Allakh-Yun tectonic zone and the Nyut-Ulbey fault (Fig. 1a). We combine them into the newly identified Late Cretaceous Severookhotsk complex.

METHODOLOGY

The mineral composition of the rocks was determined on a JSM-5480LV INCA Energy 350 scanning electron microscope with a WDS system (Jeol, Japan) at IGM SB RAS (Novosibirsk). The silicate analysis was performed in DPMGI SB RAS (Yakutsk). Rare

earth and other trace elements contents in the rocks were determined in the laboratory of analytical chemistry of the Common use center of FEGI FEB RAS (Vladivostok) by inductively coupled plasma mass spectrometry on an Agilent 8800 mass spectrometer (Agilent Techn., USA). The U-Pb, Sm-Nd, and Rb-Sr investigations were carried out in the Centre of Isotopic Research of Karpinsky Russian Geological Research Institute (Saint Petersburg). U-Th-Pb dating was performed on a SHRIMP-II SIMS. Contents and isotopic compositions of Sm, Nd, Rb, and Sr were done using the isotope dilution method on a TRITON multicollector mass spectrometer in static mode.

GEOLOGY OF THE PLUTONS AND PETROGRAPHIC-GEOCHEMICAL CHARACTERISTIC OF THE ROCKS

The Sup, Duzunya, and Batyrchan plutons are small stocks of acid and intermediate intrusive rocks with 4, 6.8, and 15 km² of square area respectively. The Sup pluton is part of the range dividing the East Khandyga River and the Sup Creek (Fig. 1b). It is located on the northern end of the Allakh-Yun tectonic zone of the South Verkhoyansk sector of the VFTB and intrudes upper Permian shallow shelf deposits, forming cordierite-bearing contact hornfelses. The Duzunya and Batyrchan plutons are in the lower reaches of the Olchan (Uolchan) River (Fig. 1c). They associate with the Nyut-Ulbey fault, which is part of the dislocations system of the major Adycha-Taryn fault (Fig. 1a). These two plutons intrude folded Upper Triassic (Norian) terrigenous (turbidite) deposits of the Kular-Nera terrane. All three plutons tend to be confined to northeast and west-east trending reverse faults with strike-slip kinematics or just strike slips. These faults are estimated as Cretaceous in age from geological data and are transversal in relation to the fold-and-thrust structures of the Allakh-Yun tectonic zone and to the Adycha-Taryn fault. Geological mapping materials mention Coniacian U-Pb age estimates for zircon (SHRIMP-II) for the rocks of the Duzunya pluton (89 \pm 1 Ma) [15], as well as for the Sup pluton (94 \pm 1 Ma) and the adjacent Kurum pluton (96 \pm 1 Ma) (unpublished data of A.V. Prokopiev) [16]. This is supported by the 94 \pm 1 Ma U-Pb (ID-TIMS) zircon age for granodiorite from the Kurum pluton [12].

The studied rocks of the Sup pluton are quartz monzodiorite and quartz monzonite, with lesser amounts of granodiorite [13]. The quartz monzodiorites and quartz monzonites are dark gray fine- and medium-grained rocks. They consist of plagioclase (up to 40 vol %), potassium feldspar (up to 35 vol %), and amphibole (~10 vol %), with augite, biotite and quartz occupying up to 5 vol % each. Plagioclase is mostly euhedral tabular grains with zoned structure with the central part consisting of andesine replaced by sericite and the rim—of oligoclase and albite. A

smaller amount of elongated plagioclase grains have polysynthetic twinning. Potassium feldspar with allotriomorphic grains has a perthitic structure, often with plagioclase inclusions. Augite has moderate values of Mg# (0.5-0.6) and a small TiO₂ admixture (up to 0.2 wt %) and forms relict fragments of small idiomorphic grains, almost completely replaced by amphibole. Amphibole composition varies from ferroan hornblende to ferroactinolite (Mg# = 0.2-0.4). Biotite varies from siderophyllite to ferrous biotite (Mg# = 0.2-0.4) and occurs along the rims of amphibole grains, forming elongated grains without any particular orientation. Quartz forms small rounded grains. Accessory and opaque minerals include apatite, zircon, epidote, ilmenite, magnetite, and leucoxene. Secondary alteration includes pelitization of potassium feldspar and chloritization of amphibole and biotite.

The Duzunya pluton is composed of granodiorite, granite, low-alkaline granite, leucocratic granite and subalkaline granite. These rocks consist of potassium feldspar and plagioclase (up to 35 vol % each), quartz (up to 20 vol %), and biotite (up to 15 vol %). Granodiorite includes individual small amphibole grains of light-brown color (up to 3 mm). Granodiorites, granites and subalkaline granites include varieties with the rapakivi texture (Fig. 2) formed by grayish-white oval potassium feldspar phenocrysts (up to 40–50 mm) with rims of plagioclase of andesine-oligoclase-albite composition (up to 3 mm), sometimes with polysynthetic twinning. These large phenocrysts contain inclusions of oval grains of potassium feldspar (15-30 mm) with plagioclase rims 0.1 to 0.5 mm wide. The plagioclase phenocrysts (up to 20 mm in size) with short-prismatic habit often have a concentric zonation of andesine-oligoclase-albite composition and are in subordinate quantities. The volume of phenocrysts in granodiorite does not exceed 20%, but increases to 60% in the more acid varieties, where they are combined with each other. The groundmass of the rock is from dark gray to black, medium-grained and consists of rounded grains of dark-gray quartz, slightly elongated subhedral plagioclase grains and allotriomorphic grains of potassium feldspar and siderophyllite (Mg# up to 0.2). Secondary alterations include pelitization of potassium feldspar, albitization and sericitization of plagioclase, chloritization and muscovitization of biotite. Accessory and opaque minerals are zircon, apatite, rutile, epidote, tourmaline, ilmenite, and magnetite.

The Batyrchan pluton consists of gray biotite-tourmaline and biotite granite and low-alkaline granite, as well as yellowish-white tourmaline subalkaline granite. The rocks are pseudoporphyritic, fine- and medium-grained. Phenocrysts of oval and tabular shape (up to 12 mm long) are mostly potassium feld-spar with tartan twin pattern and perthitic structure, sometimes with poikilitic plagioclase inclusions. Plagioclase (albite) forms both euhedral and subhedral

35 Page 4 of 9 VERNIKOVSKAYA et al.



Fig. 2. Photo of rapakivi granodiorite sample DZ-7-22 of the Duzunya pluton.

grains and occurs in the groundmass alongside allotriomorphic grains of potassium feldspar and quartz. In biotite-bearing varieties, light-brown biotite is subhedral, partially replaced by muscovite and light-green chlorite. Tourmaline is orange to light-brown, elongated, and euhedral, to a lesser extent occurs as allotriomorphic aggregates, and corresponds to a schorldravite composition (MgO up to 3.1 wt %, FeO up to 13.2 wt %). In subalkaline varieties, tourmaline occurs as individual large reabsorbed crystals (up to 8 mm) and clusters of small (up to 2 mm) allotriomorphic grains. Tourmaline features a lot of poikilitic inclusions of feldspar and apatite. Plagioclase is replaced by albite and sometimes sericite. Potassium feldspar is partially pelitized. Accessory and opaque minerals are topaz, apatite, zircon, orthite, rutile with Nb admixture (Nb₂O₅ up to 1 wt %), and ilmenite. Orthite and ilmenite forms inclusions in biotite.

By the classification in [17], the rocks of the Sup, Duzunya and Batyrchan plutons are mostly alkali-calcic and calc-alkaline series rocks. They have varying values of the K_2O/Na_2O ratio (0.4–1.7), the lowest being in the metaluminous rocks of the Sup pluton with high Na₂O content (up to 6.0 wt %) and low SiO₂ (58.6–60.4 wt %). The compositions of the Duzunya pluton rocks (SiO₂ = 64.4-73.7 wt %) vary from metaluminous to peraluminous. The Batyrchan pluton rocks ($SiO_2 = 67.4-74.6$ wt %) range from weakly to highly peraluminous. On the $FeO_{tot}/(FeO_{tot} + MgO)$ SiO₂ diagram from [17], most rocks of the Sup and Duzunya plutons plot in the ferroan trend, corresponding to A-type granites. The Batyrchan pluton rocks as well as individual samples of the Duzunya pluton correspond to magnesian varieties typical for Cordilleran type granites. The rocks of the Duzunya and Sup plutons have moderate and high Rare earth elements (REE) totals varying in the ranges 172–782 and 373–408 ppm, respectively. Their multielement spectra and REE distributions are close to those of other rapakivi-bearing formations occurring in active continental margin settings, including Aptian age rapakivi granites of the Tarbagannakh pluton in the Allakh-Yun zone of the South Verkhoyansk sector of the VFTB [7, 18, 19]. The rocks of the three studied plutons have high $(La/Yb)_N$ ratios (up to 24.2–29.5), which are close to OIB values. The Sup pluton rocks lack or display a very slight Eu anomaly (Eu/Eu* = 0.8–0.9), whereas in the other two plutons the Eu anomalies are moderate to low (Eu/Eu* = 0.1-0.4), in addition to negative Ba, Sr, and Ti anomalies. The Batyrchan pluton rocks differ in their low values of the REE total (29–74 ppm) and positive U and P anomalies, in contrast to the Duzunya and Sup pluton, which have negative P anomalies. On tectonic discrimination diagrams Nb-Y, Ta-Yb, Rb-Nb + Y, and Rb-Yb + Ta from [20], the studied rocks, including rapakivi varieties, plot in the field of granitoids that formed due to slab failure.

ISOTOPE-GEOCHRONOLOGICAL INVESTIGATIONS

We performed geochronological U—Th—Pb investigations on zircon from rocks of the Sup, Duzunya and Batyrchan pluton (Fig. 3). In quartz monzonite sample SUP-22-02 of the Sup pluton, twelve zircon grains were analyzed. The zircons are light-yellow, transparent, euhedral, prismatic to elongated crystals (369–607 μ m, $K_{\rm elon}=1.4$ –2.4) and fragments, often with inclusions, some of them fractured. On cathodoluminescence (CL) images the zircons are bright or moderately bright, show a fine zonation and elements of a sectorial structure. Grain no. 10 has a black nonzoned core (10.1) and a bright rim with fine sectorial zonation (10.2), indicating a magmatic origin. Uranium contents vary from 237 to 710 ppm, except core

10.1 (1535 ppm). Thorium contents vary from 146 to 840 ppm for 11 grains and is 1807 ppm for core 10.1. The Th/U ratio is 0.44–1.32. Results of U–Th–Pb dating for all measured zircons yielded a Concordia age of 93.5 ± 0.8 Ma, which we interpret as the crystallization age of the rock.

In low-alkaline granite sample DZ-5-22 from the Duzunya pluton, 14 grains were analyzed. The zircons are vellow, brick-red, foggy euhedral and subeuhedral prismatic to elongated crystals (335–690 μ m, K_{elon} = 2.0-3.8) and fragments with inclusions and fractures. On CL images the zircons are bright and show a twoor three-phase structure. In two-phase grains (3.1, 7.1, 7.2, 9.1, and 12.1), there are light central areas with fine zonation and dark rims with traces of zonation or black non-zonal rims. In three-phase zircons (all the others), the central area is dark with traces of fine zonation, the intermediate area is light with fine zonation, and the rim part is dark up to black. Five measurements (1.3, 6.1, 7.2, 11.2, 14.1) showed elevated uranium contents and were excluded from calculations. For the remaining 14 measurements with uranium content less than 2500 ppm (that is to say, without high-U measurements causing an overestimation of individual ages due to the matrix effect) a Concordia age of 89.5 ± 0.8 Ma was calculated, which we accept as the age of the rock.

In granodiorite sample DZ-7-22 with a welldefined rapakivi texture (Fig. 2), eleven grains were analyzed. The zircons are honey-yellow, semitransparent euhedral and subeuhedral prismatic to elongated crystals (270–636 μ m, $K_{elon} = 1.9-4.4$) and fragments with inclusions and/or fractures. On CL images, the zircons are bright and have a two- or three-phase structure. The two-phase grains have light central areas with fine zonation and black rims; in three-phase zircons (1.1, 5.1, 5.2, 8.1, 9.1, 9.2, 10.1, 11.1, 11.2), the central area is dark (up to black) with traces of a fine zonation (or without zonation), the intermediate area is light with fine zonation and the rim is from dark to black. After exclusion of the high-U measurements (2.2, 3.2, 11.2), a Concordia age of 88.2 ± 0.8 Ma was obtained. For measurements used in the calculation, the U content varies from 253 to 1582 ppm, Th content—from 87 to 600 ppm; the Th/U ratio = 0.13-0.73.

Zircon extracted from Batyrchan pluton samples of granite (BT-1/22), subalkaline granite (BT-3/22), and low-alkaline granite (BT-4/22) are significantly heterogeneous. On CL images, many grains do not have concentric growth zonation but are divided into individual domains, often with black, high-U rims. Some grains have segregated cores, many grains are significantly metamict, some have melted or rounded rims. Most obtained analyses in cores and rims are significantly discordant. Measured U–Pb ages vary from Mesoarchean to Eocene. Uranium content ranges from 27 to 5586 ppm, Th—from 3 to 1271 ppm. Some

grain rims yield early Permian ages, some others (mainly high-U)—Late Jurassic to Early Cretaceous. One spot in a high-U rim (U = 3950 ppm) from leucocratic granite sample BT-4/22 yielded an age \sim 91–89 Ma, which is close to the Concordia age obtained for zircon from the rocks of the Sup and Duzunya plutons

Sm-Nd and Rb-Sr isotopic investigations were performed for the same samples as U-Pb zircon dating. Both the one-stage and two-stage Sm-Nd model ages for the magmatic source of these rocks are Neoproterozoic and Mesoproterozoic. For Sup pluton quartz monzonite sample SUP-22-02 ($\varepsilon_{Nd}(T) = -0.6$, $(^{87}Sr/^{86}Sr)_0 = 0.705290)$ —model ages are 777 and 961 Ma respectively; for the Duzunya pluton lowalkaline granite sample DZ-5-22 ($\varepsilon_{Nd}(T) = -2.3$, $(^{87}Sr/^{86}Sr)_0 = 0.706180)$ and rapakivi granodiorite sample DZ-7-22 $(\epsilon_{Nd}(T) = -2.5, (^{87}Sr/^{86}Sr)_0 =$ 0.706199)—1.1 Ga. The latter is indicative of input of continental crustal material in the magmatic source of these rocks. On the $\varepsilon_{\rm Nd}(T)$ —(87Sr/86Sr)₀ diagram all three samples plot in the field of isotope compositions of enriched mantle sources. At the same time, the quartz monzonite sample plots in the field of Bulk Silicate Earth. We assume that the granites and subalkaline granite of the Batyrchan pluton formed with the participation of a Mesoproterozoic crustal source, whose age, according to the two-stage models is 1.4 Ga.

CONCLUSIONS

We identified a wide variety of acid and intermediate intrusive rocks for the Sup, Duzunya, and Batyrchan plutons—from monzodiorite, quartz monzonite and granodiorite to granite of normal alkalinity, low-alkaline, subalkaline, and leucocratic granites, including ones with rapakivi texture. These small intrusions located in major tectonic zones penetrated terrigenous strata of the southwestern passive continental margin of the Siberian craton. Our new U-Th-Pb data for zircon (SHRIMP-II SIMS) from acid and intermediate rocks of the Sup and Duzunya plutons, including the rapakivi varieties, show that they formed in the Cenomanian–Coniacian time 94–88 Ma. This agrees with preliminary age estimates for these intrusions [15, 16] and for Batyrchan pluton rocks. Characteristics of the geochemistry and Sn-Nd and Rb-Sr isotopy of the rocks of all three plutons indicate both an enriched mantle and a continental crustal component in their magmatic source, in which they are similar to rapakivi-bearing associations [8] formed due to slab failure in active continental margin settings. These new integrated data let us combine the rocks of the Sup, Duzunya and Batyrchan plutons and the similarly aged granitoids of the Kurum pluton into the back-arc Severookhotsk complex (94–88 Ma). These rocks formed in the back-arc of the West Okhotsk flank sector of the OCVB, on the continent, about 35 Page 6 of 9 VERNIKOVSKAYA et al.

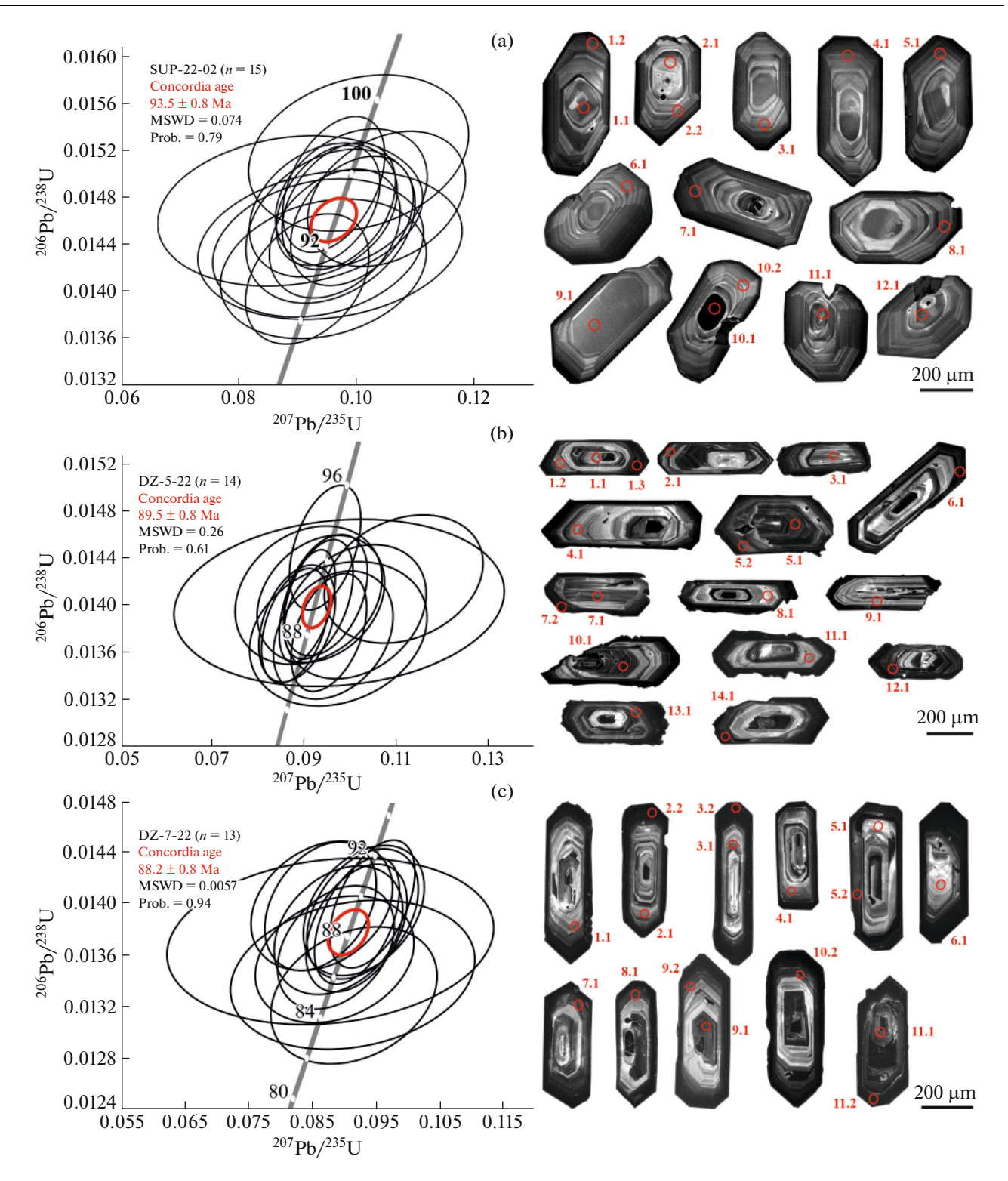


Fig. 3. Concordia diagrams and CL images of zircon from quartz monzonite sample SUP-22-02 of the Sup pluton (a) and low-alkali granite sample DZ-5-22 and granodiorite sample DZ-7-22 of the Duzunya pluton (b, c). Error ellipses are 2σ . Numbered red ovals on CL images are locations of analytical spots and their numbers in Table 1.

100–200 km inwards from the axial zone (volcanic arc). This took place after a quiescence of magmatism in this sector, somewhat preceding and then synchronously with initiation of magmatic activity in the

Okhotsk sector of the OCVB. The Late Cretaceous Severookhotsk complex magmatism became both a source and a trigger for metasomatic processes during the formation of the adjacent and coeval Sn—polyme-

	S
	Ξ
	≅
	⇉
	Ω
•	ರ
	ല
•	₫
	3
	ò
	ഉ
7	Ξ
	d
	듯
	n tron
(Η.
	\approx
_	≌
•	\overline{Z}
¢	Ξ.
	s of zirco
	S
	5
•	Ĭ
	ŭ
	읙
	S
	9
	Ē
•	e inves
	8
	5
	₹
	\mathbf{s}
•	Ξ
	۲
-	7
	ㅗ
Ē	1
·	Ĺ
۲	_
-	_
(Ξ
	š
-	ĭ
	ಷ
	S
4	Ż
7	_
_	<u>9</u>
-	₫
Ē	ď

	D2 (%)		7	-2	8-	1	-3	-1	3	-1	-1	1	0	-2	0	1	0		18	1	-5	-1	-2	9	-3	5	-1	2	0
	D1 (%)		180	-62	-229	21	-71	-14	72	-37	-39	17	-1	-56	13	34		_	438	27	-147	-28	-57	164	-83	132	-32	48	3
	(5) (2)		94.2 ± 1.5	95.6 ± 1.5	94.5 ± 1.6	90.8 ± 1.6	94.2 ± 1.5	93.2 ± 1.7	93.3 ± 1.4	92.1 ± 1.5	90.4 ± 1.5	92.7 ± 1.4	97.1 ± 1.7	94.4 ± 1.3	92.1 ± 1.7	94.6 ± 1.5	94.3 ± 1.4	. E)	90 ± 1.4	89.9 ± 1.4	93.5 ± 1.3	92.8 ± 1.4	90.3 ± 1.5	87.7 ± 1.4	88.8 ± 1.3	87.9 ± 1.3	94.6 ± 1.3	90.1 ± 1.3	91.7 ± 1.3
Age, Ma	$(1) \\ U^{2\xi\zeta}/dq^{70\zeta}$	139°10′45.3″ E	101.5 ± 5	93.2 ± 3.3	86.3 ± 8.6	91.6 ± 6.6	91.6 ± 4.8	92.7 ± 5.4	96 ± 3.9	90.7 ± 6.8	89 ± 4	93.4 ± 4.2	97.1 ± 7	92.3 ± 3.3	92.6 ± 8.5	95.9 ± 4.9	94 ± 3.6	142°45′01.3″	107.5 ± 6.4	90.8 ± 5.2	88.2 ± 2.1	91.8 ± 2.9	88.3 ± 6.1	93.4 ± 4.9	86 ± 3.2	92.5 ± 3.1	93.4 ± 2.1	91.8 ± 3.5	91.8 ± 3.6
	0.000 (1) 0.000	Ž	94.6 ± 1.5	95.4 ± 1.5	94 ± 1.7	90.8 ± 1.5	94 ± 1.5	93.2 ± 1.7	93.4 ± 1.4	92 ± 1.5	90.3 ± 1.4	92.8 ± 1.4	97.1 ± 1.7	94.3 ± 1.3	92.1 ± 1.7	94.7 ± 1.5	94.2 ± 1.4	°51'43.9" N,	91 ± 1.4	89.9 ± 1.4	93.2 ± 1.3	92.7 ± 1.4	90.2 ± 1.5	88 ± 1.4	88.6 ± 1.3	88.2 ± 1.3	94.5 ± 1.3	90.2 ± 1.3	91.7 ± 1.3
	Егг.	es: 63°0	0.3	0.4	0.2	0.2	0.3	0.3	0.4	0.2	0.4	0.3	0.2	0.4	0.2	0.3	0.4	ates: 64	0.3	0.3	9.0	0.5	0.2	0.3	0.4	0.4	9.0	0.4	9.4
	(1) \(\Omega_{8\text{EZ}}/*4\d_{90\text{D}}\)	GPS coordinates: 63°04′50.1″	0.01479 ± 1.6	0.01491 ± 1.6	0.01469 ± 1.8	0.01419 ± 1.7	0.01469 ± 1.6	0.01456 ± 1.8	0.0146 ± 1.5	0.01437 ± 1.7	0.01411 ± 1.6	0.01449 ± 1.6	0.01518 ± 1.8	0.01473 ± 1.4	0.0144 ± 1.8	0.0148 ± 1.6	0.01473 ± 1.5	te GPS coordin	0.01422 ± 1.6	0.01405 ± 1.6	0.01456 ± 1.4	0.01449 ± 1.5	0.01409 ± 1.7	0.01375 ± 1.6	0.01384 ± 1.5	0.01377 ± 1.5	0.01477 ± 1.4	0.01408 ± 1.5	0.01432 ± 1.4
ratios	(1) U ²⁵² /*dq ⁷⁰² (%±)	onite, Sup pluton (sampling site	0.1051 ± 5.2	0.0961 ± 3.7	0.0887 ± 10	0.0944 ± 7.6	0.0944 ± 5.4	0.0956 ± 6.1	0.0992 ± 4.3	0.0935 ± 7.8	0.0916 ± 4.7	0.0963 ± 4.7	0.1003 ± 7.6	0.0952 ± 3.8	0.0955 ± 9.6	0.0991 ± 5.3	0.097 ± 4.1	ite, Duzunya pluton (sampling site GPS coordinates: 64°	0.1117 ± 6.3	0.0936 ± 6	0.0908 ± 2.5	0.0946 ± 3.4	0.0909 ± 7.2	0.0963 ± 5.5	0.0884 ± 3.8	0.0953 ± 3.5	0.0963 ± 2.4	0.0946 ± 4	0.0946 ± 4.1
Isotope ratios	(1) *4q ³⁰² /*4q ⁷⁰² (1)	onite, Sup pluto	0.0515 ± 5	0.0467 ± 3.3	0.0438 ± 10	0.0482 ± 7.4	0.0466 ± 5.2	0.0476 ± 5.8	0.0493 ± 4	0.0472 ± 7.6	0.0471 ± 4.4	0.0482 ± 4.5	0.0479 ± 7.4	0.0468 ± 3.5	0.0481 ± 9.4	0.0486 ± 5.1	0.0478 ± 3.8	ite, Duzunya plu	0.0569 ± 6.1	0.0483 ± 5.8	0.04522 ± 2.1	0.0473 ± 3	0.0468 ± 7	0.0508 ± 5.3	0.0463 ± 3.6	0.0502 ± 3.2	0.0473 ± 1.9	0.0487 ± 3.7	0.0479 ± 3.8
	*°9d ₉₀₇ %	rtz monz	0.32	0.00	0.67	0.48	0.32	0.42	0.24	0.52	0.26	0.27	0.46	0.46	09.0	0.32	0.21	low-alkaline gran	1.00	0.56	0.22	0.15	0.36	0.36	0.34	0.24	0.15	0.32	1.12
	∩ _{8€Z} /Ч. _{Z€Z}	SUP-22-02, quartz monz	1.07	0.44	0.92	0.77	0.74	0.72	98.0	0.72	0.81	0.83	0.95	1.22	0.64	0.79	1.32	low-alka	0.72	0.40	0.25	0.34	0.79	0.44	0.45	0.25	0.33	0.89	0.18
mc	ЧΤ		436	232	232	211	317	279	685	250	497	443	293	1807	146	288	840	Z-5-22, I	421	220	923	333	326	187	969	300	811	298	543
Content, ppm	U	Sample	423	551	260	284	443	402	710	360	632	551	319	1535	237	379	959	Sample DZ	909	572	3784	1000	425	436	1377	1218	2569	1005	3070
Co	*dq ⁹⁰²		5.4	7.06	3.3	3.48	5.61	5.05	8.92	4.47	7.68	88.9	4.18	19.5	2.94	4.83	8.32	Š	7.48	6.94	47.4	12.5	5.16	5.17	16.4	14.4	32.6	12.2	38.2
	Analyt. spot no.		1.1	1.2	2.1	2.2	3.1	4.1	5.1	6.1	7.1	8.1	9.1	10.1	10.2	11.1	12.1		1.1	1.2	1.3*	2.1	3.1	4.1	5.1	5.2	6.1*	7.1	7.2*

Table 1. (Contd.)

		D2 (%)	5	7	-3	10	4-	-2	0	-3		-1	9-	4-	-2	-1	5	-3	1	3	1	9-	1	7	1	-1	0
		D1 (%)	142	191	-92	249	-103	-46	12	-79		-26	-171	66-	-53	-17	127	-75	27	84	33	-177	18	09	33	-38	-3
		(2)	89.5 ± 1.8	87.7 ± 1.6	88.7 ± 1.3	88.7 ± 1.5	98.9 ± 1.3	89.7 ± 1.3	89.9 ± 1.3	93.4 ± 1.3	"E)	86.9 ± 1.3	89.9 ± 1.3	91.7 ± 1.3	88.4 ± 1.3	93.6 ± 1.3	84.9 ± 1.4	87.9 ± 1.6	88.4 ± 1.3	86 ± 1.5	89.1 ± 1.3	89.8 ± 1.3	88.7 ± 1.3	89.5 ± 1.3	89.2 ± 1.3	87.6 ± 1.2	91.3 ± 1.2
Age, Ma	$U^{\xi\xi\zeta}/dq^{\eta\zeta}$	95 ± 14	94.4 ± 7.3	85.7 ± 2.8	97.8 ± 5.8	94.8 ± 1.9	88.1 ± 2.4	90.3 ± 2.9	90.5 ± 2.5	142°45′04.1	86.1 ± 4.8	84.2 ± 4.2	88.2 ± 1.8	86.7 ± 3.8	92.9 ± 1.9	88.9 ± 5	85.5 ± 9.8	89.3 ± 3	88.7 ± 7.3	90.2 ± 3.3	84 ± 3.4	89.4 ± 2.5	91.6 ± 2.5	90.4 ± 3.6	86.3 ± 3.5	91.2 ± 1.5	
		(1) U ⁸⁶² /dq ⁸⁰²	89.8 ± 1.8	88.1 ± 1.6	88.5 ± 1.3	89.3 ± 1.5	98.7 ± 1.3	89.6 ± 1.2	89.9 ± 1.3	93.2 ± 1.3	'51'36.4" N,	86.9 ± 1.3	89.5 ± 1.3	91.5 ± 1.2	88.3 ± 1.3	93.5 ± 1.3	85.1 ± 1.4	87.8 ± 1.7	88.4 ± 1.3	86.1 ± 1.5	89.1 ± 1.3	89.5 ± 1.3	88.8 ± 1.3	89.6 ± 1.3	89.3 ± 1.3	87.5 ± 1.2	91.3 ± 1.2
		Еп.	0.1	0.2	0.4	0.3	0.7	0.5	0.4	0.5	nates: 64	0.3	0.3	9.0	0.3	9.0	0.3	0.2	0.4	0.2	0.4	0.4	0.5	0.5	0.4	0.3	0.8
		(1) U ⁸⁶² /*dq ⁹⁰² (1)	0.01402 ± 2.1	0.01376 ± 1.8	0.01383 ± 1.4	0.01394 ± 1.7	0.01543 ± 1.4	0.01399 ± 1.4	0.01405 ± 1.5	0.01457 ± 1.4	ite GPS coordir	0.01357 ± 1.5	0.01399 ± 1.5	0.01429 ± 1.4	0.01379 ± 1.5	0.01461 ± 1.4	0.01329 ± 1.6	0.01371 ± 1.9	0.01381 ± 1.5	0.01345 ± 1.8	0.01392 ± 1.5	0.01398 ± 1.5	0.01387 ± 1.4	0.014 ± 1.4	0.01395 ± 1.5	0.01366 ± 1.4	0.01427 ± 1.4
	ratios	(1) U ²⁸² /*dq ⁷⁰² (%±)	0.098 ± 15	0.0974 ± 8.1	0.088 ± 3.4	0.1011 ± 6.2	0.0978 ± 2.1	0.0907 ± 2.8	0.093 ± 3.3	0.0932 ± 2.9	ton (sampling s	0.0885 ± 5.8	0.0865 ± 5.2	0.0908 ± 2.2	0.0891 ± 4.6	0.0958 ± 2.2	0.0916 ± 5.8	0.088 ± 12	0.0919 ± 3.5	0.0913 ± 8.6	0.0929 ± 3.9	0.0863 ± 4.2	0.092 ± 3	0.0944 ± 2.9	0.0931 ± 4.2	0.0887 ± 4.2	0.094 ± 1.7
	Isotope ratios	(1) *4d ⁹⁰² /*4d ⁷⁰² (1)	0.0505 ± 15	0.0513 ± 7.9	0.0462 ± 3.1	0.0526 ± 6	0.046 ± 1.5	0.047 ± 2.4	0.048 ± 3	0.0464 ± 2.6	ite, Duzunya pluton (sampling site GPS coordinates: 64°51'36.4" N	0.0473 ± 5.6	0.0448 ± 5	0.04607 ± 1.7	0.0468 ± 4.4	0.04756 ± 1.7	0.05 ± 5.6	0.0465 ± 12	0.0483 ± 3.2	0.0492 ± 8.4	0.0484 ± 3.6	0.0448 ± 3.9	0.0481 ± 2.6	0.0489 ± 2.5	0.0484 ± 3.9	0.0471 ± 3.9	$11.2* 85.2 6953 1295 0.19 0.02 0.04779 \pm 1.1 0.094 \pm 1.7 0.01427 \pm 1.4 0.8 91.3 \pm 1.2 91.2 \pm 1.5 91.3 \pm 1.2 -3 0$
		*°9d ₉₀₇ %	1.27	0.61	0.22	0.43	0.20	0.27	0.19	0.24	ranodior	0.29	0.63	0.24	0.35	0.16	0.39	1.01	0.27	0.73	0.25	0.47	0.13	0.17	0.23	0.20	0.02
		∩ _{8ЕZ} /Ч.СЕZ	0.51	0.47	0.40	0.43	0.25	0.29	0.25	0.25	-7-22, rapakivi granodioi	0.37	0.27	0.17	0.41	0.17	0.32	0.35	0.17	0.40	0.30	0.36	0.39	0.32	0.28	0.32	0.19
	ım	ЧΤ	82	113	490	168	1137	733	293	627		405	330	924	384	928	145	87	222	134	354	515	009	484	231	439	1295
,	Content, ppm	Ω	166	250	1266	403	4620	2576	1229	2612	Sample DZ	1129	1242	5673	696	5597	463	253	1322	344	1210	1493	1582	1551	845	1399	6953
	S	*4 q ⁹⁰²	2.02	2.97	15.1	4.84	61.4	31.1	14.9	32.8	Sa	13.2	15	8.69	11.5	70.4	5.3	3.01	15.7	4.01	14.5	18	18.9	18.7	10.1	16.5	85.2
		Analyt. spot no.	8.1	9.1	10.1	11.1	11.2*	12.1	13.1	14.1*	=	1.1	2.1	2.2*	3.1	3.2*	4.1	5.1	5.2	6.1	7.1	8.1	9.1	9.2	10.1	11.1	11.2*

Pb_c and Pb*—common and radiogenic lead, respectively. Repetition accuracy (1G) was 0.44%. Err. corr.—error correlation. Common lead was corrected both for measured ²⁰⁴Pb (1) and ²⁰⁶Pb/²³⁸U and ²⁰⁶Pb/²³⁸U and ²⁰⁷Pb/²³⁸U and ²⁰⁷Pb/²³⁸U and ²⁰⁷Pb/²³⁸U and ²⁰⁷Pb/²³⁸U and ²⁰⁷Pb/²³⁸U ages, *—High—U measurements excluded from calculation.

2025

tallic and Au—Bi mineralization in the Allakh-Yun tectonic zone. The latter reflects the importance of studying rapakivi-bearing formations for understanding the origin of ore processes.

FUNDING

This work was financially supported by the Russian Science Foundation (grant no. 24-17-00057).

CONFLICT OF INTEREST

The authors of this work declare that they have no conflicts of interest.

REFERENCES

- L. M. Parfenov and B. A. Natal'in, Tectonophysics 127, 291–304 (1986). https://doi.org/10.1016/0040-1951(86)90066-1
- 2. Tectonics, Geodynamics, and Metallogeny of the Sakha Republic (Yakutia), Ed. by L. M. Parfenov and M. I. Kuz'min (Nauka, Moscow, 2001) [in Russian].
- L. M. Parfenov, N. A. Berzin, A. I. Khanchuk, G. Bardach, V. G. Belichenko, A. N. Bulgatov, S. I. Dril', G. L. Kirillova, M. I. Kuz'min, W. J. Nokleberg, A. V. Prokopiev, V. F. Timofeev, O. Tomurtogoo, and H. Yang, Russ. J. Pac. Geol. 22 (6), 7–41 (2003).
- L. M. Parfenov, Continental Margins and Island Arcs of the Mesozoides of the Northeast of Asia (Nauka, Novosibirsk, 1984) [in Russian].
- 5. S. D. Sokolov, Geotectonics **44** (6), 493–510 (2010). https://doi.org/10.1134/S001685211006004X
- V. Fridovskii, A. Vernikovskaya, N. Matushkin, P. Kadilnikov, M. Kudrin, and Ya. Tarasov, in *Proc.* 13th Sci.-Pract. Conf. Geology and Mineral and Raw Material Resources of Northeastern Russia (Ammosov North-Eastern Federal Univ., Yakutsk, 2023), pp. 343– 348 [in Russian].
- A. E. Vernikovskaya, V. Y. Fridovsky, N. V. Rodionov, N. Yu. Matushkin, P. I. Kadilnikov, M. V. Kudrin, and Ya. A. Tarasov, Dokl. Earth Sci. **514** (2), 391–400 (2024). https://doi.org/10.1134/S1028334X23602869
- F. Hu, S. Liu, W. Zhang, Z. Deng, and Chen Xu, Lithos 262, 486–506 (2016). https://doi.org/10.1016/j.lithos.2016.07.034
- 9. V. V. Akinin and E. L. Miller, Petrology **19** (3), 237–277 (2011). https://doi.org/10.1134/S0869591111020020
- V. F. Polin, P. L. Tikhomirov, A. I. Khanchuk, and A. V. Travin, Dokl. Earth Sci. 497 (2), 273–280 (2021).
- 11. A. V. Prokopiev, A. S. Borisenko, G. N. Gamyanin, V. Yu. Fridovsky, L. A. Kondrat'eva, G. S. Anisimova,

- V. A. Trunilina, E. A. Vasyukova, A. I. Ivanov, A. V. Travin, O. V. Koroleva, D. A. Vasiliev, and A. V. Ponomarchuk, Russ. Geol. Geophys. **59** (10), 1237–1253 (2018). https://doi.org/10.1016/j.rgg.2018.09.004
- I. V. Chernyshev, A. G. Bakharev, N. S. Bortnikov, Yu. V. Goltsman, A. B. Kotov, G. N. Gamyanin, A. V. Chugaev, E. B. Sal'nikova, and E. D. Bairova, Geol. Ore Deposits 54 (6), 411–433 (2012). https://doi.org/10.1134/S1075701512060049
- A. P. Babich, L. A. Krukovskaya, and A. L. Porkunova, The 1: 200 000 State Geological Map of the Russian Federation, Ser. Yudoma, Sheet No. P-54-VIII (Eastern Khandyga River), Explanatory Note (Moscow Branch Karpinsky Russ. Geol. Res. Inst., Moscow, 2016).
- 14. R. Yu. Nurgaleev, *The 1:200 000 State Geological Map of the Russian Federation, 2nd ed., Ser. Yana—Indigirka, Sheet No. Q-54-XXIX, XXX (Predporozhnyi)* (Moscow Branch Karpinsky Russ. Geol. Res. Inst., Moscow, 2016).
- G. Kh. Protopopov, A. M. Trushelev, and Yu. V. Kuznetsov, The 1: 1000000 State Geological Map of the Russian Federation, 3rd ed., Ser. Upper Yana—Kolyma, Sheet no. Q-54-Ust'-Nera,, Explanatory Note (Karpinsky Russ. Geol. Res. Inst., St. Petersburg, 2019).
- G. G. Kazakova, A. F. Vas'kin, A. P. Kropachev, O. I. Shcherbakov, A. V. Prokop'ev, A. K. Khudolei, L. A. Sharov, T. K. Ivanova, V. K. Kuz'min, O. V. Zheleboglo, and V. I. Makar, *The 1:1000 000 State Geological Map of the Russian Federation, 3rd ed., Ser. Upper Yana–Kolyma, Sheet No. R-54-Oimyakon,, Explanatory Note* (Kartfabr. Karpinsky Russ. Geol. Res. Inst., St. Petersburg, 2013).
- B. R. Frost, C. G. Barnes, W. J. Collins, R. J. Arculus, D. J. Ellis, and C. D. Frost, J. Petrol. 42, 2033–2048 (2001). https://doi.org/10.1093/petrology/42.11.2033
- 18. D. Gagnevin, J. S. Daly, and G. Poli. Lithos **78** (1–2), 157–195 (2004). https://doi.org/10.1016/j.lithos.2004.04.043
- X. X. Wang, T. Wang, A. Castro, R. Pedreira, X. X. Lu, and Q. H. Xiao, Lithos 126, 369–387 (2011). https://doi.org/10.1016/j.lithos.2011.07.007
- 20. J. B. Whalen and R. S. Hildebrand, Lithos **348–349**, 105179 (2019). https://doi.org/10.1016/j.lithos.2019.105179

Publisher's Note. Pleiades Publishing remains neutral with regard to jurisdictional claims in published maps and institutional affiliations. AI tools may have been used in the translation or editing of this article.